J Neurophysiol 103: 3526–3534, 2010.
First published April 21, 2010; doi:10.1152/jn.00105.2010.

Removal of Movement Artifact From High-Density EEG Recorded During Walking and Running

Joseph T. Gwin,[1] Klaus Gramann,[2] Scott Makeig,[2] and Daniel P. Ferris[1]

[1]*Human Neuromechanics Laboratory, School of Kinesiology; University of Michigan, Ann Arbor, Michigan; and* [2]*Swartz Center for Computational Neuroscience, Institute for Neural Computation; University of California, La Jolla, California*

Submitted 25 January 2010; accepted in final form 15 April 2010

Gwin JT, Gramann K, Makeig S, Ferris DP. Removal of movement artifact from high-density EEG recorded during walking and running. *J Neurophysiol* 103: 3526–3534, 2010. First published April 21, 2010; doi:10.1152/jn.00105.2010. Although human cognition often occurs during dynamic motor actions, most studies of human brain dynamics examine subjects in static seated or prone conditions. EEG signals have historically been considered to be too noise prone to allow recording of brain dynamics during human locomotion. Here we applied a channel-based artifact template regression procedure and a subsequent spatial filtering approach to remove gait-related movement artifact from EEG signals recorded during walking and running. We first used stride time warping to remove gait artifact from high-density EEG recorded during a visual oddball discrimination task performed while walking and running. Next, we applied infomax independent component analysis (ICA) to parse the channel-based noise reduced EEG signals into maximally independent components (ICs) and then performed component-based template regression. Applying channel-based or channel-based plus component-based artifact rejection significantly reduced EEG spectral power in the 1.5- to 8.5-Hz frequency range during walking and running. In walking conditions, gait-related artifact was insubstantial: event-related potentials (ERPs), which were nearly identical to visual oddball discrimination events while standing, were visible before and after applying noise reduction. In the running condition, gait-related artifact severely compromised the EEG signals: stable average ERP time-courses of IC processes were only detectable after artifact removal. These findings show that high-density EEG can be used to study brain dynamics during whole body movements and that mechanical artifact from rhythmic gait events may be minimized using a template regression procedure.

INTRODUCTION

A noninvasive method for recording human electrocortical brain dynamics during mobile activities could have far-reaching benefits (Makeig et al. 2009). Cognitive neuroscientists exploring embodied cognition could study brain dynamics associated with cognitive processes during whole body interactions within natural environments. Studies of human motor control would no longer be limited to studies of constrained movements. Bioengineers might be able to use such a method to derive control signals for neurorehabilitation and prosthetic technologies. An unanswered question in neuroscience is to what extent human cortex participates in the generation of rhythmic motor behaviors, in particular those motor behaviors associated with locomotion. The answer seems to lie in a multifaceted control strategy including descending, peripheral, and central control (Yang and Gorassini 2006). An ability to measure brain dynamics during locomotion may provide additional information regarding the significance of descending control.

EEG is the only noninvasive brain imaging modality that uses sensors that are light enough to wear during locomotion and have sufficient time resolution to record brain activity on the time scale of natural motor behavior. However, EEG has historically been considered to be too noise prone to allow such recordings. Mechanical artifact in EEG signals, associated with head movements during locomotion, can have amplitude that is an order of magnitude larger than the underlying brain related EEG signals.

A similar phenomenon occurs during simultaneous EEG and functional MRI (fMRI). In this situation, alternating magnetic fields (gradients) of the MR scanner cause large repetitive artifact in EEG signals. Artifact template subtraction procedures have been used successfully to remove fMRI gradient artifact from EEG signals (Allen et al. 2000). Unlike fMRI gradient artifact, which is relatively invariant over time (Garreffa et al. 2004), mechanical artifact associated with locomotion is time varying. Kinematics and kinetics of human walking exhibit both short-term (step to step) and long-term (over many steps) variability (Hausdorff et al. 1995, 1996; Jordan et al. 2006, 2007). Time-varying sources of EEG noise, such as the ballistocardiogram artifact in EEG recorded in a strong magnetic field, have been extracted from EEG signals using channel-based template subtraction procedures and subsequent spatial filtering (Debener et al. 2005, 2007). This combined method was shown to be more effective than channel-based template subtraction (Niazy et al. 2005) or spatial filtering (Benar et al. 2003; Eichele et al. 2005) alone.

Here, we implemented a two-step approach to removing locomotion-induced mechanical artifact in high-density EEG signals recorded while subjects walked and ran on a treadmill while simultaneously performing a visual oddball discrimination task. We first removed stride phase-locked mechanical artifact using a channel-based template regression procedure. To address slow fluctuations (over many strides) in the time profile of the gait-related artifact, we used moving time-window averaging of the stride phase-locked data to compute an artifact template for each stride and each channel. To address step-to-step fluctuations in the phase and amplitude of the gait-related artifact resulting from variability in gait kinematics and kinetics, we regressed out the artifact template signals from each EEG signal. Next, we applied an adaptive independent component analysis (ICA) mixture model algorithm (AMICA) (Palmer et al. 2006, 2008), generalizing infomax (Bell and Sejnowski 1995; Lee et al. 1999a), and multiple mixture (Lee et al. 1999b; Lewicki and Sejnowski 2000) ICA

Address for reprint requests and other correspondence: J. T. Gwin, 401 Washtenaw Ave., Ann Arbor, MI, 48109 (E-mail: jgwin@umich.edu).

approaches, to parse EEG signals into spatially static, maximally independent component (IC) processes (Makeig et al. 1996).

Unlike more spatially stationary artifacts in EEG signals arising from eye movements, scalp muscles, fMRI gradients, etc. (Debener et al. 2005, 2007; Jung et al. 2000a,b), which may be resolved by ICA decomposition into a subspace of one or more ICs, we found that gait-related movement artifact remained in many if not most of the independent components. This prevented us from removing only a small subset of components capturing the movement artifacts. Instead, we applied the template regression procedure (previously applied to the channel data) to the IC processes, reversed the time-warping to produce artifact-reduced ICs, and applied the ICA mixing matrix to recover a second set of artifact-reduced EEG signals.

To evaluate the combined effects of channel-based and channel-based plus component-based artifact removal, we computed the power spectral density of the resulting signals and compared spectral power in the 1.5- to 8.5-Hz frequency band before and after artifact removal, finding no sign of overcorrection of the EEG signals. We also compared the artifact-reduced stimulus event-related potentials (ERPs) in walking and running conditions to uncorrected ERPs recorded while standing. For the walking conditions, ERPs that were nearly identical to ERPs while standing were visible before and after applying noise reduction. For the running condition, stable ERPs were only detectable after artifact removal.

METHODS

Subjects

Eight healthy volunteers with no history of major lower limb injury and no known neurological or locomotor deficits completed this study (7 males and 1 female; age range, 21–31 yr). All subjects provided written informed consent before the experiment. All procedures were approved by the University of Michigan Internal Review Board and complied with the standards defined in the Declaration of Helsinki.

Task

Subjects stood, walked (0.8 and 1.25 m/s), and ran (1.9 m/s) on a force measuring treadmill facing a monitor placed at eye level ~1 m in front of them. Standard (80%) and oddball (20%) stimuli (vertical or 45° rotated black crosses on a white background, respectively) were displayed for 500 ms. The stimuli occupied about 75% of the display area (14° of visual angle). The interstimulus interval between successive presentations varied randomly between 500 and 1,500 ms. For each gait condition (standing, slower walking, faster walking, running), subjects performed two experimental blocks. In the first block, subjects were asked to press a button on a wireless Wii controller (Nintendo, Kyoto, Japan) held in their right hand whenever the target (oddball) stimulus appeared. In the second block, subjects were asked to silently count the number of target stimuli presented, without producing a manual response. Each session began with the standing condition, followed by the other three conditions in random order. The standing blocks lasted 5 min each, whereas walking and running blocks lasted 10 min each.

Recording brain and body dynamics

EEG was recorded using a compact ActiveTwo amplifier and 248-channel active electrode array (BioSemi, Amsterdam, The Netherlands). Electrodes were affixed to the scalp using a custom made whole head cap (Fig. 1). During the experimental setup, electrode impedance was measured, and electrode gel was used to ensure that the impedance was <20 KΩ for each channel. EEG signals were sampled at 512 Hz and after collection were high-pass filtered above 1 Hz. All processing and analysis was performed in Matlab (The Mathworks, Natick, MA) using scripts based on EEGLAB 7.1.4 (//www.sccn.ucsd.edu/eeglab), an open source environment for processing electrophysiological data (Delorme and Makeig 2004).

For two of eight subjects, EEG signals could not be recorded during the running condition because the electrode cap did not stay in place during running (i.e., it was too big for the subject). For the remaining six subjects, channels exhibiting substantial noise throughout the collection were removed from the data in the following manner. First, channels with SD $>1{,}000$ μV were removed; then any channel whose kurtosis was >5 SD from the mean was removed; finally, channels that were uncorrelated ($r < 0.4$) with nearby channels for $>1\%$ of the time samples were removed. On average, 130 EEG channel signals were retained after visual inspection and removal of noisy channels (range, 89–164; SD, 24.6). The data were re-referenced off-line to the average of the remaining channels. Visual stimulus events were delivered, and their latencies were incorporated into the EEG data stream using DataSuite (A. Vankov, //www.sccn.ucsd.edu/wiki/DataSuite).

Subjects walked and ran on a custom built, dual-belt, force measuring treadmill with two 24-in-wide belts mounted flush with the floor (Collins et al. 2009). The distance between the belts was 0.75 in. The average belt speed variation while adult subjects walk on this treadmill at 1.25 m/s is 1.8%. The lowest natural frequency of the force treadmill is 41 Hz (for mediolateral forces). Each belt has a separate force platform mounted as its base for measuring ground

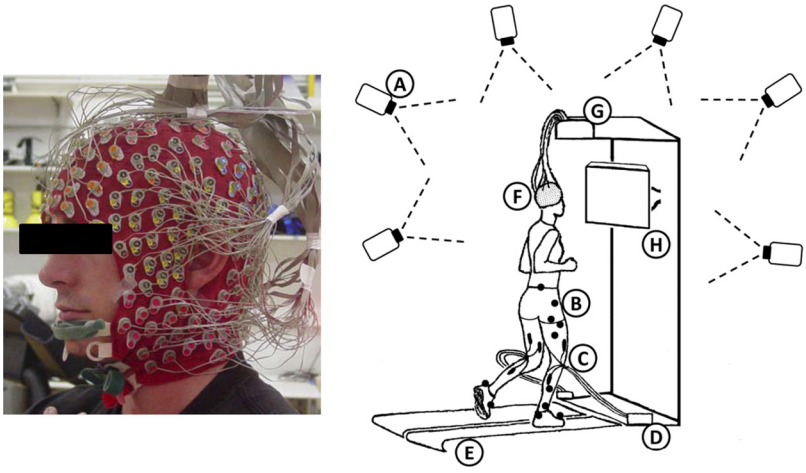

FIG. 1. *Left*: subject wearing a custom whole head 248-channel electrode cap. *Right*: a sketch of the experimental setup showing (*A*) motion capture cameras and (*B*) markers, (*C*) lower limb EMG (not used in this study), (*D*) the EMG amplifier, (*E*) the dual-belt in-ground force measuring treadmill, (*F*) the electrode head-cap, (*G*) the EEG amplifier, and (*H*) the display for the visual stimuli.

reaction forces for each leg independently, with a sample rate of 1,200 Hz.

We used an eight-camera, 120 frames/s, motion capture system (Motion Analysis, Santa Rosa, CA) to record the position of 25 reflective markers (low-pass filtered at 6 Hz to remove movement artifact) on the lower limbs and pelvis. From these marker positions, the kinematics of the ankle, knee, and hip joints were computed using Visual-3D software (C-Motion, Germantown, MD). Event detection algorithms within Visual-3D were used to determine when heel strikes occurred based on vertical ground reaction forces. If force platform signals were compromised because the subject drifted across the centerline of the dual belt treadmill, a kinematic-based pattern recognition technique within Visual-3D was used to identify heel strikes (Stanhope et al. 1990).

Removal of gait-related movement artifact

EEG signals were epoched, time-locked to single gait cycles (left heel strike to left heel strike), and linearly time-warped using EEGLAB processes (Makeig et al. 2007) so that, after time-warping, heel strike events (left then right) occurred at the same adjusted latencies in each epoch. For each channel and each stride, a gait-related artifact template was created by averaging the neighboring 20 time-warped stride-locked epochs (10 future epochs and 10 past epochs). This artifact template was linearly scaled to best fit the time-warped EEG signal in a least-squares sense and was subtracted from the data to form artifact-reduced time-warped data. These cleaned data were reverse time-warped to produce artifact-reduced continuous time EEG channel signals. We refer to this process as channel-based artifact removal (Fig. 2).

In addition, we performed ICA decomposition on the concatenated single-trial data (including all experimental conditions) for each subject separately using AMICA. Before performing ICA decomposition, time periods of EEG with substantial artifact, based on the z-transformed power across all channels at a given time-point being >0.8, were rejected using EEGLAB. The rejected frames were inspected visually, and regions of <50 accepted frames between any two sets of rejected frames were also rejected. The resulting ICA unmixing matrix was multiplied with the cleaned EEG channel signals, giving a set of maximally independent component (IC) process time courses. These ICs were subjected to the same noise reduction algorithm that was first applied to the channel data. Multiplying the further artifact-reduced ICs by the ICA mixing matrix (the inverse of the unmixing matrix) resulted in a second set of further cleaned EEG channel signals. We refer to this process as IC-based artifact removal (Fig. 2).

Power spectral density

For each gait condition (standing, slower walking, faster walking, running) and each method of artifact removal (before artifact removal, after channel-based removal, after further IC-based removal), we computed the power spectral density for each EEG channel using Welch's method. For illustrative purposes, we computed the power spectral envelope for each subject, defined as the maximum and minimum spectral density at each frequency over all EEG channels. We analyzed spectral power in the 1.5- to 8.5-Hz range to assess the efficacy of the gait-related artifact removal methods. This frequency band was selected because *1*) in all gait conditions for all subjects, it encompassed the step frequency and the first two harmonics of the step frequency; *2*) its lower cut-off (1.5 Hz) was greater that the high-pass filter cut-off frequency (1 Hz) that was applied to all EEG signals before analysis; and *3*) frequencies >8.5 Hz accounted for $<6\%$ of the total spectral power in the artifact templates for all gait conditions (slow walking, 6.2%; faster walking, 5.1%; running, 5.5%; Fig. 3).

We used a 4-by-1 analysis of covariance (ANCOVA) to assess changes in the power spectra of the EEG signals across gait conditions before performing gait-related artifact removal. Spectral frequency was treated as a covariate. To test the hypothesis that the gait-related artifact removal procedures would decrease the spectral power in the EEG signals for all locomotion conditions (slower walking, faster walking, and running), we used the same ANCOVA model and introduced method of artifact removal (before artifact removal, after channel-based removal, after further IC-based removal) as a repeated measure. All statistical analysis was performed in SPSS 17.0 (SPSS, Chicago, IL). Significance was set at $\alpha = 0.05$ a priori. Bonferroni correction was used to address the problem of multiple comparisons.

Stimulus-locked ERPs

EEG signal epochs were extracted, time-locked from -600 to $+1{,}000$ ms relative to visual stimulus onsets. Epochs containing artifacts not related to locomotion (such as eye movements and line

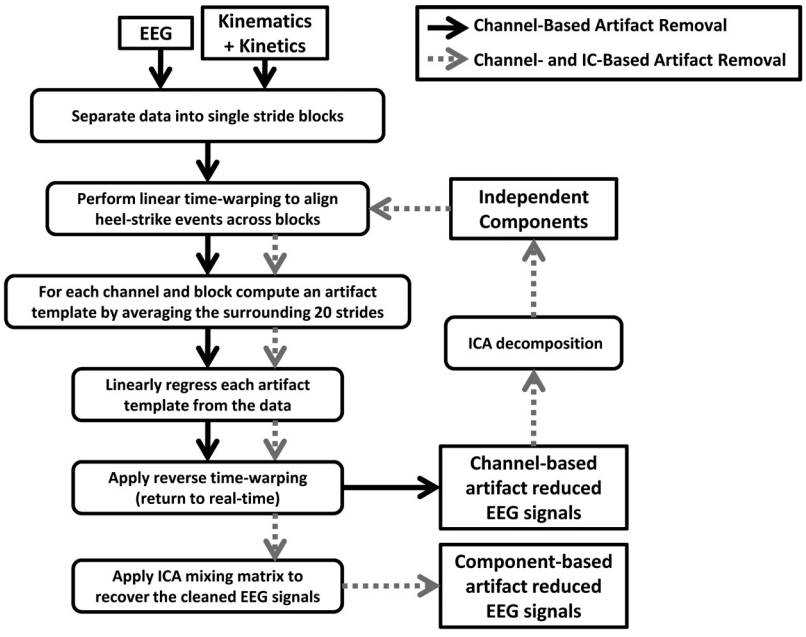

FIG. 2. Flow chart of the channel-based (solid black arrows) and component-based (dotted gray arrows) artifact removal procedures. For component-based artifact removal, the independent components were derived from channel-based artifact removed EEG signals.

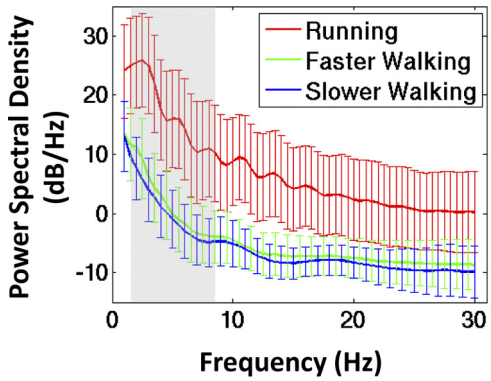

FIG. 3. Grand average power spectral density (±SD) of the independent component (IC)-based artifact templates that were removed from the EEG signals during walking at 0.8 m/s (blue line), walking at 1.25 m/s (green line), and running at 1.9 m/s (red line). The shaded region indicates the frequency band (1.5–8.5 Hz) used in subsequent statistical analyses.

noise) were excluded from further analysis using EEGLAB routines that determined the probability of occurrence of each trial by computing the probability distribution of EEG channel signals. Epochs with a probability of occurrence >3 SD from the mean across all epochs were rejected from further analysis (Delorme et al. 2007). The remaining epochs were averaged to form EEG channel-based ERPs. Additionally, these epochs were multiplied by the ICA unmixing matrix to form IC activity epochs and averaged across epochs to form IC-based ERPs.

Here, an alternative approach would have been to remove ocular, electrocardiac, and other non–gait-related artifacts using ICA (Jung et al. 2000a,b). However, if ICA-based artifact removal techniques had been implemented, it would have been difficult to isolate the effects of the template regression procedure on the channel power spectra from the effects of ICA-based artifact removal techniques. The artifact rejection procedure that we implemented ensured that gait-related artifact, which was present in all trials, remained, whereas other artifact events such as eye blinks and line noise were minimized in the data analyzed.

Next, ICs were clustered across subjects using EEGLAB routines implementing k-means clustering on vectors jointly coding differences in IC scalp maps, power spectra, and ERPs; the resulting joint vector was reduced to 10 principal dimensions using principal component analysis (PCA) (Gramann et al. 2009; Jung et al. 2001). Previous analysis of a similar visual oddball discrimination task for seated subjects showed that brain processes projecting maximally to the frontal midline would contribute substantially to the ERP, particularly to the postmotor positivity (Makeig et al. 2004). Visualizations of grand average IC-based ERPs confirmed that the mediofrontal IC cluster (comprised of components projecting maximally to the frontal midline) had a clear and substantial stimulus-locked ERP. Additionally, at least one IC from each subject was contained in this cluster. Therefore the ICs in the mediofrontal cluster were selected for further analysis of the artifact removal procedures. For all ICs in the mediofrontal cluster, each gait condition, and each stage of artifact removal, we computed stimulus-locked IC-based ERPs and compared their time profiles across conditions.

RESULTS

Power spectral density of the recorded EEG signals increased with step frequency (Fig. 4). A 4-by-1 ANCOVA, with spectral frequency (1.5–8.5 Hz) as the covariate, showed significant differences in spectral power across gait conditions before gait-related artifact removal [$F(3,1) = 14{,}824$, $P < 0.001$]. Grand mean spectral powers were 3.45, 4.43, 5.49, and 65.01 μV^2/Hz during standing, slow walking, faster walking, and running, respectively. In the running condition, the amplitude of EEG signals before artifact removal could be an order of magnitude larger than after artifact removal (Fig. 5).

The gait-related artifact removed was quasi-periodic at the stride frequency. The most pronounced gait-related artifacts tended to be 180° out of phase with vertical center-of-mass displacement as estimated from the displacement of motion-capture markers on the pelvis (Gard et al. 2004). However, spectral power in the gait-related artifact template was not isolated to the mean step frequency and its harmonics. This likely reflects the complex dynamic interaction between the EEG sensors, the EEG wires, the head cap, and the head, as well as to step-to-step variations in stride duration. For example, stride duration varied from roughly 720 to 800 ms for the running subject shown in Fig. 6. In addition, the amplitude of the movement artifact steadily increased over many strides. The template regression procedure was developed to account for these slow (over many strides) and fast (stride-to-stride) fluctuations in gait-related artifact (Fig. 6). After performing removal of gait-related artifact, the EEG signals appeared much cleaner (Fig. 6).

To evaluate the effects of the artifact removal procedures on the EEG signal power spectra, we introduced artifact removal method into our ANCOVA model as a repeated measure. Across all gait conditions, spectral power in the EEG signals decreased with each iteration of the artifact removal procedure [$F(2,1) = 16{,}797$, $P < 0.001$]. In both walking conditions (0.8 and 1.25 m/s), gait-related artifact removed from the EEG signals was minimal (Fig. 7, *A* and *B*). However, in the running condition (1.9 m/s), the EEG signals exhibited substantial increases in spectral power across a broad spectrum and particularly at the mean step frequency and its harmonics. This artifact was reduced but not eliminated by the channel-based and IC-based artifact rejection procedures (Fig. 7*C*). After IC-based artifact removal, the grand mean spectral powers were 3.5, 3.9, and 31.7 μV^2/Hz for slow walking, faster walking, and running, respectively. The differences in the grand mean spectral power between the standing condition and the movement conditions remained significant for running ($P < 0.001$) and fast walking ($P < 0.001$) but not for slow walking ($P = 0.756$). There was a significant interaction between subject and artifact removal method [$F(5,2) = 644$, $P < 0.001$]. Specifically, further decreases in spectral power after IC-based removal (compared with spectral power after channel-based artifact removal) were evident for some (3) but not all (6) subjects (Fig. 8).

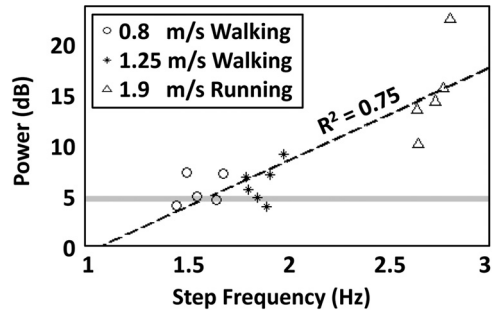

FIG. 4. Average spectral power in the 1.5- to 8.5-Hz band for each subject and each gait condition plotted vs. the subject-specific step frequency: walking at 0.8 m/s (circle), walking at 1.25 m/s (star), and running at 1.9 m/s (triangle). The gray horizontal line indicates the grand mean spectral power in the 1.5- to 8.5-Hz range for the standing condition. The black dashed line indicates a best fitting line through the data ($R^2 = 0.75$).

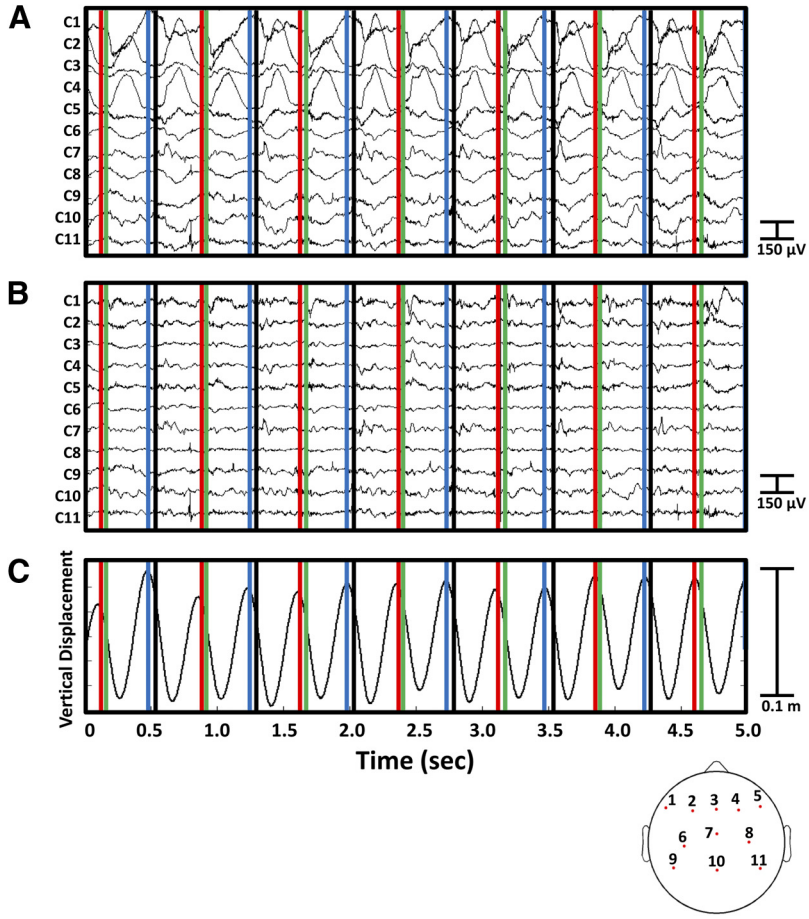

FIG. 5. A 5-s sample of EEG data from a representative subject running at 1.9 m/s (*A*) before and (*B*) after performing channel-based and IC-based artifact removal. The corresponding vertical center-of-mass displacement is shown in *C*. Vertical lines indicate left toe off (red), right heel strike (green), right toe off (blue), and left heel strike (black). *Bottom*: topographical layout of the 11 displayed EEG channels.

EEG signal epochs were extracted from −600 ms before to +1,000 ms after visual stimulus onsets; these epochs were averaged to form EEG channel ERPs. In the running condition, channel ERPs appeared cleaner after gait-related artifact removal than before artifact removal (Fig. 9).

In both walking conditions, ERPs time-locked to visual target (oddball) stimulus onsets for ICs in the mediofrontal cluster, before and after artifact removal, appeared similar in time profile and amplitude to ERPs for the same ICs recorded in the standing condition. Before artifact removal, the amplitudes and time profiles of the IC ERPs in the running condition did not resemble those in the standing condition; after artifact removal, the IC ERPs in the running and standing conditions appeared similar (Fig. 10).

DISCUSSION

To our knowledge, this is the first study of EEG and ERPs from a cognitive task recorded during human locomotion. Our results show the feasibility of removing gait-related movement artifact from EEG signals so that electrocortical processes that are associated with cognitive, motor, or perceptual tasks performed during locomotion can be studied. Specifically, we showed that by using high-density EEG

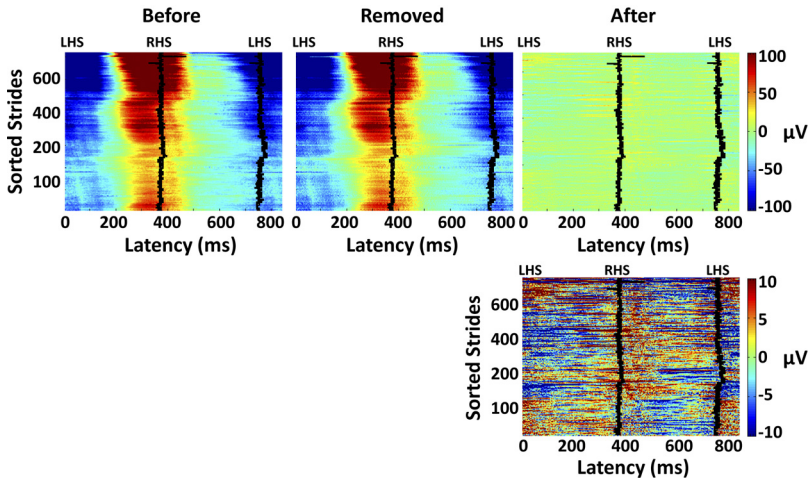

FIG. 6. Single-stride EEG signals at channel C1 (Fig. 5) during running at 1.9 m/s for a representative subject, plotted as color-coded horizontal lines smoothed with a (vertical) moving average of 5 strides. Strides are sorted chronologically; 0 latency represents a left heel strike (LHS) and the solid traces represent the latency of the next right and then left heel strikes (RHS and LHS, respectively). *Top left*: the EEG signals before artifact removal. *Top middle*: the gait-related artifact templates removed. *Top right*: the EEG signals remaining after channel- and IC-based artifact removal. *Bottom right*: the EEG signals remaining shown on a 10-times finer color scale than the *top panels*.

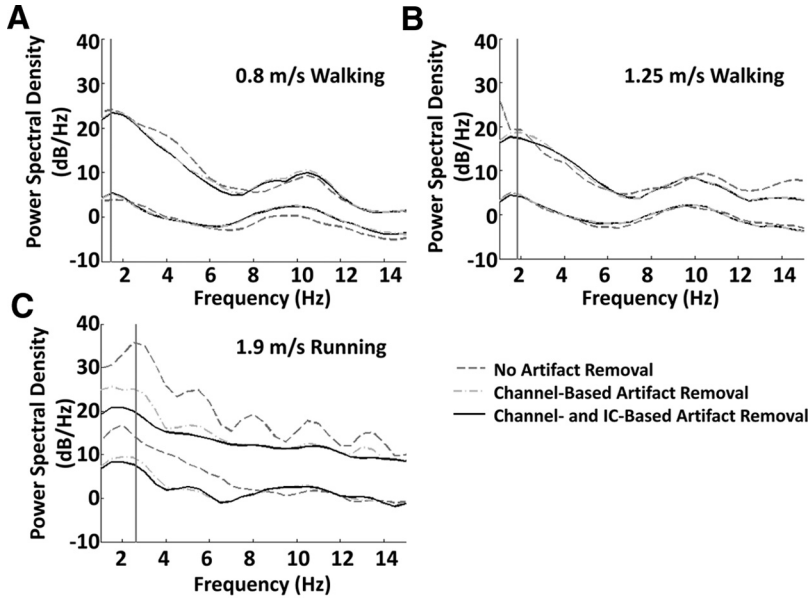

FIG. 7. EEG channel power spectral density envelopes (max and min channel spectra): before artifact removal (dashed line), after performing channel-based artifact removal (dash-dot line), and after performing IC-based artifact removal for a representative subject (*A*) walking at 0.8 m/s, (*B*) walking at 1.25 m/s, and (*C*) running at 1.9 m/s (solid line). Gray vertical lines indicate the mean step frequency in each condition.

recordings with (≤248) active electrodes synchronized to motion capture and mechanical force measurements, it is possible to analyze EEG and derived ERP signals during walking and that for a visual oddball task, these have similar continuous and event-related dynamics as in a standing subject condition. Furthermore, in a more active locomotor condition (1.9 m/s running), we showed successful application of artifact removal techniques that take into account the time-varying nature of the gait-related artifact to separate brain EEG signals from gait-related noise. In the running condition, similar average ERP time-courses of IC processes were only detectable after artifact removal.

To do this, we modified existing artifact removal techniques, designed for time-invariant noise sources (Allen et al. 2000), and applied them to EEG signals containing time-varying gait-related movement artifact. The artifact removal method that we implemented was intended to remove artifacts that were phase-locked to the gait cycle. Other artifacts (e.g., line noise, eye movement, and muscle activities) were not removed by these means. These artifacts can be addressed by other methods, such as by identifying ICs that explain the portions of the EEG associated with these processes (Jung et al. 2000a,b).

The artifact removal method implemented here involved *1*) performing a linear time-warping procedure to align heel strike events to a common latency template before performing artifact removal, *2*) computing an artifact template for each stride based on the surrounding 20 strides, *3*) using linear regression to fit a channel-based artifact template to the recorded signals for each stride, *4*) performing ICA decomposition on the continuous data, *5*) using linear regression to remove a component-based artifact template from recorded signals for each stride, *6*) applying reverse time warping to the artifact-reduced component signals, and *7*) applying the ICA mixing matrix to recover the artifact-reduced channel signals (Fig. 2). We found that, in three of the six subjects, applying the second stage of artifact removal (IC-based artifact removal, steps 4–7 above) provided a clear further reduction in gait-related movement artifact. The head cap may have fit some subjects better than others, and the running mechanics of certain subjects may have lead to more dramatic head accelerations. Nevertheless, it is not entirely clear why these further reductions were evident in some but not all subjects.

The artifact removal method that we implemented requires considerable computational resources. To run ICA, enough

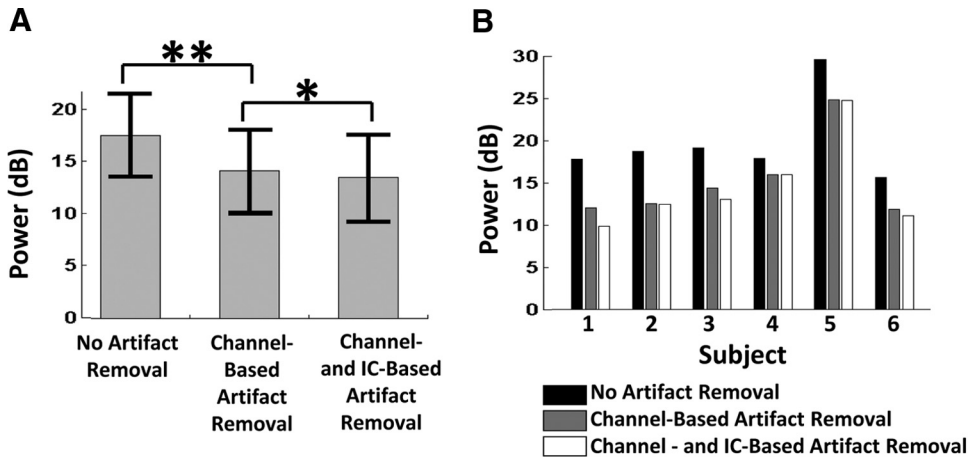

FIG. 8. During 1.9 m/s running, (*A*) grand mean spectral power in the 1.5- to 8.5-Hz band for all channels and subjects and (*B*) for all channels for each subject separately: before artifact removal (black); after channel-based artifact removal (gray); and after subsequent IC-based artifact removal (white). Error bars show ±SD. $*P < 0.01$; $**P < 0.001$.

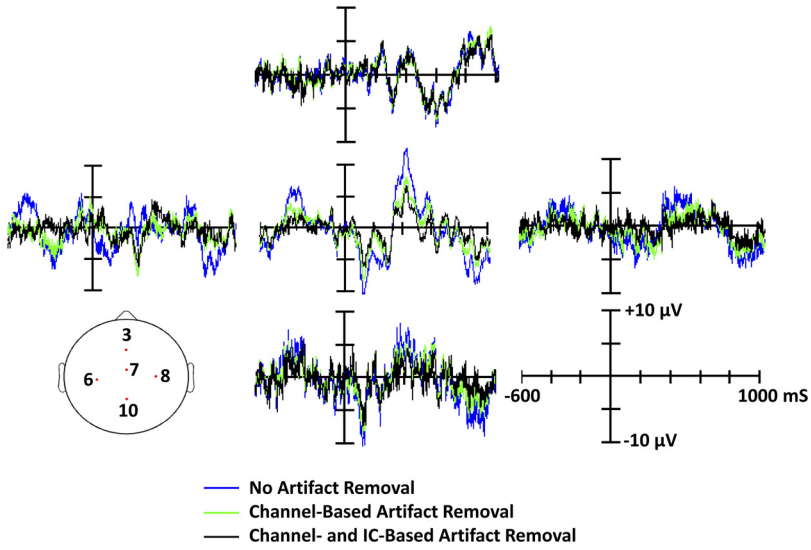

FIG. 9. Mean target event-related potentials (ERPs) of 5 EEG channels from a representative subject during running at 1.9 m/s. The scalp locations of the 5 EEG channels are shown in the *bottom left*. In each panel, 3 stages of analysis are shown: before artifact removal (blue trace); after performing channel-based artifact removal (green trace); and after subsequent IC-based artifact removal (black trace). Zero latency represents the onset of the visual target stimulus.

RAM must be available to load all EEG signals for each subject into the Matlab workspace (≤248 channels × 512 samples/s × 70 min, occupying 2 GB in single precision). Using 16-GB nodes of a compute cluster, we encountered no memory problems. AMICA is designed to run in parallel over several nodes and computation time scales near-linearly with the number of nodes available. By processing in parallel over eight nodes, we were able to run AMICA for each subject overnight.

Although 248 channels of EEG were recorded for each subject, on average only 130 channels were retained for analysis. A contributing factor here was that only a single electrode cap was available. Whereas attempts were made to recruit subjects with appropriately sized heads, in some cases, the head cap was too large for the subject (particularly in the posterior neck region). Because of unresolvable artifact caused by loose electrode placements, particularly noticeable in the running condition, 55 of the 248 electrodes were rejected >75% of the time; these electrodes were highly concentrated in the posterior neck region. The custom head cap was designed to cover regions of the head and neck below the level of the inion (Fig. 1). This design was useful for recording neck muscle contributions to ongoing EEG in looking and pointing tasks (Gramann et al. 2009; Makeig et al. 2009), but it was not optimal for recording EEG during locomotor tasks, because it did not allow the head and posterior neck portions of the cap to move with respect to each other.

There are many areas for further study that arise from the work presented here. We used active electrodes for this study that passed high-level signals through the electrode cables. Undoubtedly, passive electrodes would be more prone to movement artifacts arising from cable sway. Whether the artifact removal method that we implemented could be used to remove movement artifact from EEG recorded with passive electrodes during walking and running should be studied. In addition, wireless EEG systems, now in development in many places, would likely reduce, but likely not eliminate, movement artifact. When possible, the artifact removal method proposed here should be re-evaluated using wireless electrodes. Furthermore, we selected a 20-stride moving window for the artifact template because we found that this provided enough steps to generate a smooth template yet was still sensitive to the long-term (over many steps) variations in the

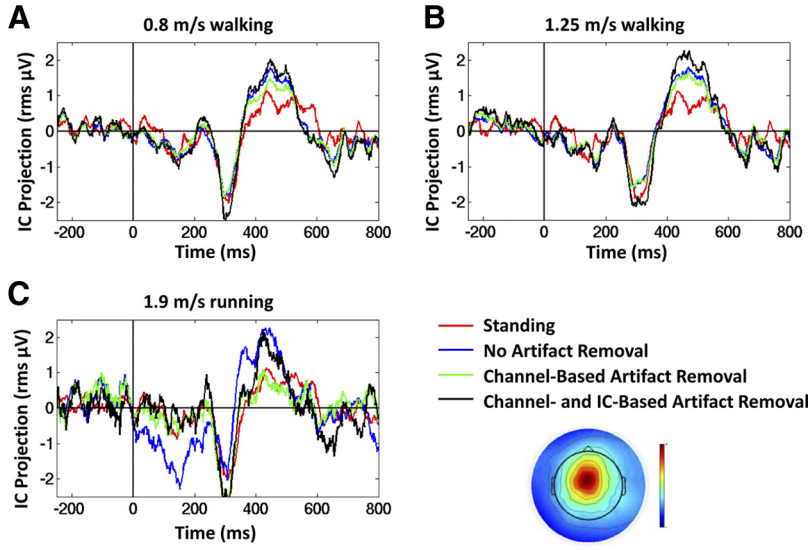

FIG. 10. Mean target ERP of a mediofrontal IC from a representative subject. The scalp topography of the selected IC is shown below the legend. Traces show ERPs in 3 gait conditions: (*A*) walking at 0.8 m/s; (*B*) walking at 1.25 m/s; and (*C*) running at 1.9 m/s. In each panel, the ERP while standing is shown (red traces) along with ERPs in 3 stages of analysis: before artifact removal (blue traces); after performing channel-based artifact removal (green traces); and after subsequent IC-based artifact removal (black traces). Zero latency represents the onset of the visual target stimulus. Vertical axis units: root-mean square microvolt projection of the IC process to all scalp electrodes.

movement artifact. Further parametric analysis to determine the optimal number of strides to include in the artifact template is recommended. Finally, we applied the artifact removal method to EEG collected during a visual oddball task. Future studies should examine other types of tasks.

We evaluated the efficacy of the procedure on EEG collected during treadmill walking and running, relatively rhythmic motor tasks. However, the artifact removal procedure we implemented is not inherently limited to removing quasi-rhythmic motor artifacts. It may be possible to use a related procedure to remove mechanical artifact from bio-electric signals recorded during other locomotor tasks, such as tasks involving rapid directional changes or responses to ground perturbations, provided enough trials are available for creation of an appropriate set of artifact templates and movement-related kinematic signals are available for performing appropriate time-warping. Here, a simple stride-order based moving average template was effective. In conditions involving locomotor challenges, extraction of mean templates might for instance be based on moving averages of trials sorted by challenge as well as time on task. Furthermore, if head kinematics were recorded and synchronized to the EEG data stream in real time, it might be possible to perform mechanical artifact removal on-line, with a delay limited only by the duration of the mechanical artifact template. These are avenues of inquiry worthy of pursuit.

Mobile recordings of EEG signals during natural behaviors may provide a foundation for further exploration into the complex links between distributed brain dynamics and motivated natural behavior. Makeig et al. 2009 proposed a wearable mobile brain/body imaging (MoBI) system and new data-driven analysis methods to model the complex resulting data. The artifact removal procedures shown here may enable the use of MoBI in more dynamic environments than previously thought.

ACKNOWLEDGMENTS

We thank E. Anaka, A. Sipp, and S. Weiss (University of Michigan) for help during data collection and A. Vankov (University of California, San Diego) for adapting his DataSuite software to synchronize our EEG and visual stimulus recordings.

GRANTS

This work was supported by Office of Naval Research Grant N000140811215, a gift from The Swartz Foundation (Old Field, NY), and an Air Force Office of Scientific Research National Defense Science and Engineering Graduate Fellowship.

DISCLOSURES

No conflicts of interest are declared by the authors.

REFERENCES

Allen PJ, Josephs O, Turner R. A method for removing imaging artifact from continuous EEG recorded during functional MRI. *Neuroimage* 12: 230–239, 2000.

Bell AJ, Sejnowski TJ. An information-maximization approach to blind separation and blind deconvolution. *Neural Comput* 7: 1129–1159, 1995.

Benar C, Aghakhani Y, Wang Y, Izenberg A, Al-Asmi A, Dubeau F, Gotman J. Quality of EEG in simultaneous EEG-fMRI for epilepsy. *Clin Neurophysiol* 114: 569–580, 2003.

Collins SH, Adamczyk PG, Ferris DP, Kuo AD. A simple method for calibrating force plates and force treadmills using an instrumented pole. *Gait Posture* 29: 59–64, 2009.

Debener S, Strobel A, Sorger B, Peters J, Kranczioch C, Engel AK, Goebel R. Improved quality of auditory event-related potentials recorded simultaneously with 3-T fMRI: removal of the ballistocardiogram artefact. *Neuroimage* 34: 587–597, 2007.

Debener S, Ullsperger M, Siegel M, Fiehler K, von Cramon DY, Engel AK. Trial-by-trial coupling of concurrent electroencephalogram and functional magnetic resonance imaging identifies the dynamics of performance monitoring. *J Neurosci* 25: 11730–11737, 2005.

Delorme A, Makeig S. EEGLAB: an open source toolbox for analysis of single-trial EEG dynamics including independent component analysis. *J Neurosci Methods* 134: 9–21, 2004.

Delorme A, Sejnowski T, Makeig S. Improved rejection of artifacts from EEG data using high-order statistics and independent component analysis. *Neuroimage* 34: 1443–1449, 2007.

Eichele T, Specht K, Moosmann M, Jongsma ML, Quiroga RQ, Nordby H, Hugdahl K. Assessing the spatiotemporal evolution of neuronal activation with single-trial event-related potentials and functional MRI. *Proc Natl Acad Sci USA* 102: 17798–17803, 2005.

Gard SA, Miff SC, Kuo AD. Comparison of kinematic and kinetic methods for computing the vertical motion of the body center of mass during walking. *Hum Mov Sci* 22: 597–610, 2004.

Garreffa G, Bianciardi M, Hagberg GE, Macaluso E, Marciani MG, Maraviglia B, Abbafati M, Carni M, Bruni I, Bianchi L. Simultaneous EEG-fMRI acquisition: how far is it from being a standardized technique? *Magn Reson Imaging* 22: 1445–1455, 2004.

Gramann K, Onton J, Riccobon D, Mueller H, Bardins S, Makeig S. Human brain dynamics accompanying use of egocentric and allocentric reference frames during navigation. *J Cogn Neurosci* In press.

Hausdorff JM, Peng CK, Ladin Z, Wei JY, Goldberger AL. Is walking a random walk? Evidence for long-range correlations in stride interval of human gait. *J Appl Physiol* 78: 349–358, 1995.

Hausdorff JM, Purdon PL, Peng CK, Ladin Z, Wei JY, Goldberger AL. Fractal dynamics of human gait: stability of long-range correlations in stride interval fluctuations. *J Appl Physiol* 80: 1448–1457, 1996.

Jahn K, Deutschlander A, Stephan T, Kalla R, Hufner K, Wagner J, Strupp M, Brandt T. Supraspinal locomotor control in quadrupeds and humans. *Prog Brain Res* 171: 353–362, 2008.

Jordan K, Challis JH, Newell KM. Long range correlations in the stride interval of running. *Gait Posture* 24: 120–125, 2006.

Jordan K, Challis JH, Newell KM. Walking speed influences on gait cycle variability. *Gait Posture* 26: 128–134, 2007.

Jung TP, Makeig S, Humphries C, Lee TW, McKeown MJ, Iragui V, Sejnowski TJ. Removing electroencephalographic artifacts by blind source separation. *Psychophysiology* 37: 163–178, 2000a.

Jung TP, Makeig S, Westerfield M, Townsend J, Courchesne E, Sejnowski TJ. Removal of eye activity artifacts from visual event-related potentials in normal and clinical subjects. *Clin Neurophysiol* 111: 1745–1758, 2000b.

Jung TP, Makeig S, Westerfield M, Townsend J, Courchesne E, Sejnowski TJ. Analysis and visualization of single-trial event-related potentials. *Hum Brain Mapp* 14: 166–185, 2001.

Lee TW, Girolami M, Sejnowski TJ. Independent component analysis using an extended infomax algorithm for mixed subgaussian and supergaussian sources. *Neural Comput* 11: 417–441, 1999a.

Lee TW, Lewicki MS, Girolami M, Sejnowski TJ. Blind source separation of more sources than mixtures using overcomplete representations. *IEEE Signal Processing Letter* 6: 87–90, 1999b.

Lewicki MS, Sejnowski TJ. Learning overcomplete representations. *Neural Comput* 12: 337–365, 2000.

Makeig S, Bell AJ, Jung TP, Sejnowski TJ. Independent component analysis of electroencephalographic data. *Adv Neural Inform Process Syst* 8: 145–151, 1996.

Makeig S, Delorme A, Westerfield M, Jung TP, Townsend J, Courchesne E, Sejnowski TJ. Electroencephalographic brain dynamics following manually responded visual targets. *PLOS Biol* 2: 747–762, 2004.

Makeig S, Gramann K, Jung TP, Sejnowski TJ, Poizner H. Linking brain, mind and behavior. *Int J Psychophysiol* 73: 95–100, 2009.

Makeig S, Onton J, Sejnowski T, Poizner H. Prospects for mobile, high-definition brain imaging: spectral modulations during 3-D reaching. *Neuroimage* 36, Suppl. 1, 2007.

Miyai I, Tanabe HC, Sase I, Eda H, Oda I, Konishi I, Tsunazawa Y, Suzuki T, Yanagida T, Kubota K. Cortical mapping of gait in humans: a near-infrared spectroscopic topography study. *Neuroimage* 14: 1186–1192, 2001.

Niazy RK, Beckmann CF, Iannetti GD, Brady JM, Smith SM. Removal of FMRI environment artifacts from EEG data using optimal basis sets. *Neuroimage* 28: 720–737, 2005.

Norton JA. Higher neural control is required for functional walking. *Clin Neurophysiol* 119: 2675–2676, 2008.

Palmer JA, Kreutz-Delgado K, Makeig S. Super-Gaussian mixture source model for ICA. In: *Lecture Notes in Computer Science*, edited by Rosca J, Erdogmus D, Principe JC, Haykin S. Springer, 2006, p. 854–861.

Palmer JA, Makeig S, Kreutz-Delgado K, Rao BD. Newton method for the ICA mixture model. Proceedings of the 33rd IEEE International Conferance on Acoustics and Signal Processing, Las Vagas, Nevada, March 30 to April 4, 2008.

Stanhope SJ, Kepple TM, McGuire DA, Roman NL. Kinematic-based technique for event time determination during gait. *Med Biol Eng Comput* 28: 355–360, 1990.

Yang JF, Gorassini M. Spinal and brain control of human walking: implications for retraining of walking. *Neuroscientist* 12: 379–389, 2006.

Yogev-Seligmann G, Hausdorff JM, Giladi N. The role of executive function and attention in gait. *Mov Disord* 23: 329–342, 2008.